On the advances to obtain excellent and repeatable mechanical properties and build quality of LaserForm® Ti gr23 (A) across whole build platform

Anthony Beckers[1], Gokula Krishna Muralidharan[1], Karel Lietaert[1], Nachiketa Ray[1], Pierre Van Cauwenbergh[1], Koen Vanacken[1], Lore Thijs[1], Jonas Van Vaerenbergh[1]

[1]*3D Systems Leuven, Grauwmeer 14, B-3001, Leuven, Belgium*

Direct Metal Printing (DMP) or Laser Based Powder Bed Fusion (L-BPF) enables manufacturing of highly complex geometries which are used in a wide range of applications - healthcare to aerospace. Producing these products with excellent and consistent part quality in terms of density and mechanical properties is key. DMP ProX® 320 machine has been used for over 10 years for this purpose. In this study, the key improvements made on the process stability for targeting consistent build quality across build platform and repeatability have been evaluated. The quality is assessed by determining the density, mechanical properties and surface roughness of direct metal printed LaserForm® Ti gr23 (A). The main finding from the study is that the use of the optimized gas flow enables production of LaserForm® Ti gr23 (A) with consistent and improved mechanical properties across the whole build platform. Moreover, there is no need any more for hot isostatic pressing to ensure good fatigue properties. The elongation strain to failure increased by 15 % to 20 %, which is 4-5 % higher than ASTM F3001 specifications. The axial fatigue limit ($5x10^6$ loading cycles) was 637 MPa (R=0.1), which is as good as or even better than annealed wrought Ti6Al4V.

Keywords: Direct Metal Printing (DMP), Laser Based Powder Bed Fusion (L-PBF), DMP ProX 320, LaserForm® Ti Gr23 (A), mechanical properties, fatigue

Introduction

Laser Based Powder Bed Fusion (L-BPF) is an Additive Manufacturing (AM) technique, which selectively fuses powder particles to build an object layer-by-layer based on a CAD model [1]. L-PBF Ti-6Al-4V components are having a huge scope in aerospace and healthcare applications because of the alloy's intrinsic properties such as biocompatibility and high strength-to-weight ratio [1,2]. However, both aerospace and healthcare are fatigue critical applications and emphasizes the critical

importance of providing these industries reliable build quality of L-PBF Ti-6Al-4V components with excellent and repeatable quasi-static as well as dynamic mechanical properties [1].

Although the AM technology has matured well in the last decades with significant progresses made on the L-PBF process optimization, literature still shows a significant scatter of ductility as well as fatigue performance of L-PBF Ti-6Al-4V [1,2]. This scatter has been mostly attributed to the presence of material defects such as pores and surface roughness, residual stresses and the presence of harmful brittle phases or undesired microstructural morphologies [1–3]. The review article by Li et al. [2] reported ductility values ranging from 4% to 13% and fatigue limits (R=0.1, 10^6 cycles) ranging from 400 MPa to 600 MPa for L-PBF Ti-6Al-4V samples which underwent heat treatment and concomitant surface treatment [2]. It is worth to note that similar material features control the mechanical performance of conventionally produced Ti-6Al-4V as well [2]. Consensus exists in literature that these material defects act as major stress concentrators and thus are the primary contributors to the observed scatter in the data of mechanical properties of L-PBF Ti-6Al-4V [1,2]. These material defects are commonly induced by either L-PBF machine instabilities or the use of sub-optimal process parameters.

This work aims at performing a critical assessment of DMP ProX® 320 LaserForm® Ti gr23 (A) to prove the stability of the DMP ProX® 320 machine and the performance of the optimized LaserForm® Ti gr23 (A) parameters to obtain homogeneous, reliable and repeatable quasi-static and dynamic mechanical properties.

Materials and methods

Tensile and fatigue test coupons were manufactured via L-PBF on a 3D Systems DMP ProX® 320 machine equipped with a 500 W fiber laser using LaserForm® Ti Gr23 (A) powder. Table 1 shows the chemical composition of the powder. Cylindrical test coupons were printed in 30, 60 and 90 µm layer thickness and were positioned across the base plate. The samples were stress relieved according to the advised heat treatment from 3D Systems.

Table 1: Chemical composition of LaserForm® Ti Gr23 (A).

Material	**Ti**	**Al**	**V**	**N**	**C**	**H**	**Fe**	**O**	**Y**	**Others**
LaserForm® Ti Gr23 (A)	Bal.	5.5-6.5	3.5-4.5	≤0.03	≤0.08	≤0.012	≤0.25	≤0.13	≤0.005	≤0.4

Tensile testing was performed in an accredited external lab according to the ASTM E8M standard for the evaluation of quasi-static mechanical properties. Cylindrical samples were printed and machined to ASTM E8M specimen type 4.

Fatigue testing was performed according to the ASTM E466 standard using standard specimens with minimum diameter of 6 mm and radius 50 mm. An Instron 8801 with a 100 kN dynamic load cell was used for the high cycle fatigue testing. A force controlled constant amplitude uni-axial cyclic loading was carried out with a load ratio R = 0.1. The test was performed in air at 23±2°C at a frequency of 25 Hz up to failure or $5x10^6$ cycles. The cyclic loading was performed at several loads in order to obtain the fatigue curve and fatigue limit.

The oxygen content in the printed parts was measured by Inert Gas Fusion (IGA) analysis according to the ASTM E1409 standard. The bulk density of the printed part was measured by Archimedes density according to the ASTM B962 standard. Sample preparation for microstructural analysis was done by grinding followed by OPS with colloidal silica suspension and addition of H_2O_2. The samples were etched during 6 seconds with a modified Keller's reagent consisting of 25 ml HNO_3, 5 ml HF and 50 ml H_2O. The microstructure was observed by Light Optical Microscopy (LOM) with a Nikon Eclipse MA100.

Improved reliability and repeatability of material properties of LaserForm® Ti Gr23.

Obtaining reliable and repeatable properties in L-PBF of Ti-6Al-4V is not just dependent on process parameters but also on powder characteristics (oxygen content), gas flow, choice of heat treatments and homogeneity across the build platform – supported by a robust machine design.

Oxygen content

Ti gr 23 is an extra low interstitial variant of the Ti-6Al-4V type of alloys. The interstitial elements like oxygen are kept as low as possible in order to obtain improved ductility and fatigue properties [4,5]. Ti has a high affinity to O_2 and is temperature dependent. During DMP, the powder bed locally reaches temperatures above 400 °C, thus creating a high risk for O_2 pick up by the powder. To counter this, DMP ProX® 320 machine's vacuum chamber concept serves very useful. The system performs a vacuum pre-cycle prior to the job and actively removes air and moisture from the build chamber and the powder bed, and fills it afterwards with inert argon gas. The oxygen and moisture extraction from the powder feed gives a boiling effect (Figure 1). The efficient vacuum pre-cycle helps achieve extremely low O_2 contents (< 25 ppm) in the build chamber. Furthermore, the leak tight design of the

vacuum chamber ensures that no O_2 can leak in the build chamber and results in a very low argon consumption during printing. This key vacuum chamber concept thereby helps to eliminate the risks for oxygen pick up by the powder, and ensures an excellent shelf life of the powder. Figure 2 shows the powder oxygen evolution from a powder batch which was used in the same machine for over 9 months. The O_2 level in the powder stays in the range 0.09 – 0.12 wt % throughout the entire period of time proving the advantage of the vacuum chamber concept. By maintaining such clean atmosphere for the powder handling and together with the careful parameter optimization, excellent and repeatable print-to-print quality can be achieved.

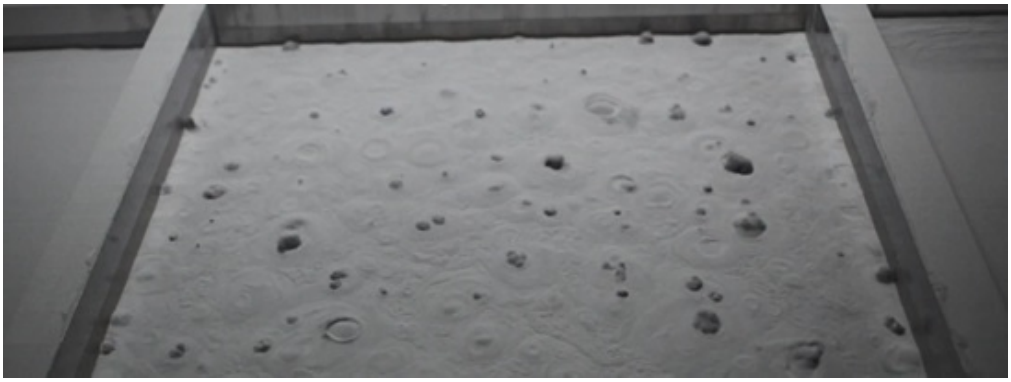

Figure 1- Boiling effect showing the extraction of O2 and moisture from the powder feed

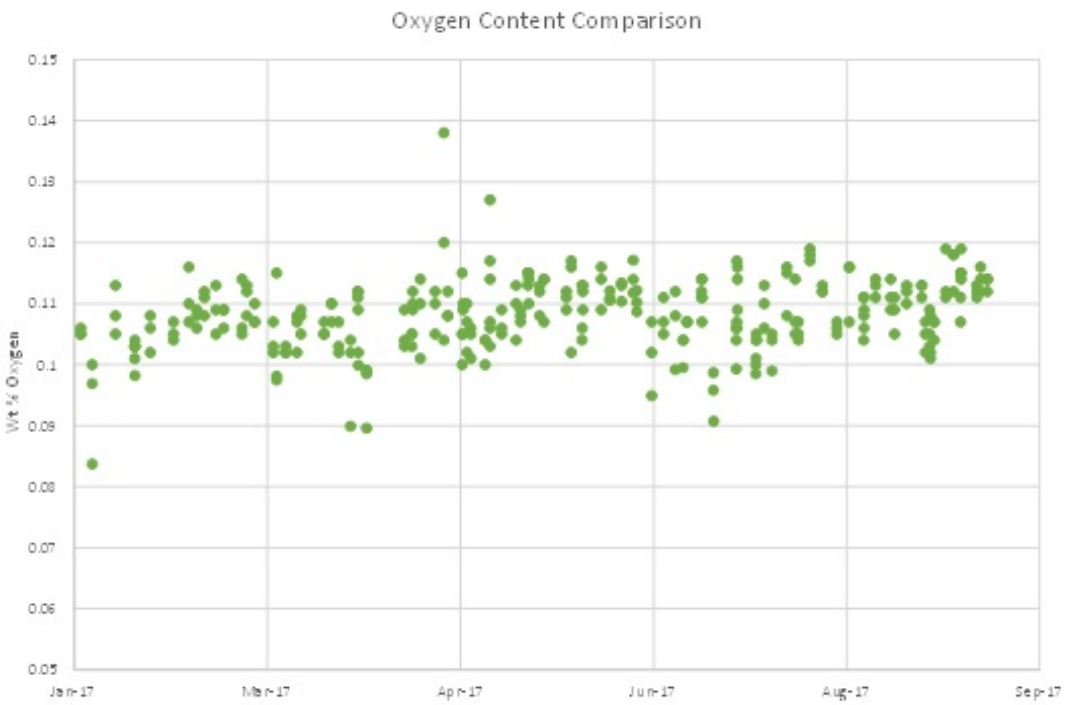

Figure 2 - Change in O2 in the powder over a period of 9 months

Gas flow

Gas flow across the powder bed has a significant effect on the print quality of the material. Direct metal printing is a localized welding of powder at high speeds. The process produces several local events such as vapor plume, denudation zones, spatter and condensates which majorly affect the printing quality [6–8]. Vapor plumes are generated above the melt due to the application of high energy laser on the powder bed. This vapor plume – if not removed properly – absorbs partially the laser energy, thus leading to incomplete welding and non-fusion defects. Denudation zones are formed due to the high velocity circular flow of the melt driven by the Maragoni flow. These zones attract un-molten particles near the melt pool and create a depression around the melt zone. This results in non-uniform melting and pore formation [9]. Spatters and condensates on the other hand are produced as secondary products during the fast localized melting which results in deposits on the already printed parts or on the non-molten powder bed as the laser progresses. Depending on the size and location of these spatters and condensates, the deposition quality of the powder bed is affected and thereby creates process related defects. The widely accepted reason for the formation of spatters has been mostly related to the recoil pressure of the meltpool, the Marangoni effect and the entrainment of

particles due to the flow of the vapor plumes above the meltpool [10–12]. The sources of the spatters have been classified as hot entrainment ejections, cold entrainment ejections and recoil pressure induced droplet break up ejections [11]. The size of the spatters are defined by the type of entrainment process and ranges from 10 to 100 um, depending on the type of material being processed [6,12]. All of these spatters have a huge influence on the defects formation during the printing process.

Therefore, a stable gas flow across the powder bed (Figure 3(a)) combined with a well optimized process parameters can ensure a stable meltpool and efficient vapor extraction above the meltpool. Most of the commercial metal printers have a gas flow system for this purpose. Figure 3(b) shows the visual impression on the effect of bad flow on the surface quality of the printed part. The XY plane surface roughness of the printed parts using a bad flow condition easily varies from 15 to 150 Ra (um) compared to 5 – 7 Ra (um) for parts printed with well optimized flow. Figure 4 shows a comparison plot of the elongation of machined tensile test coupons, which were printed in different sample sizes, using a bad gas flow and using optimized gas flow conditions.

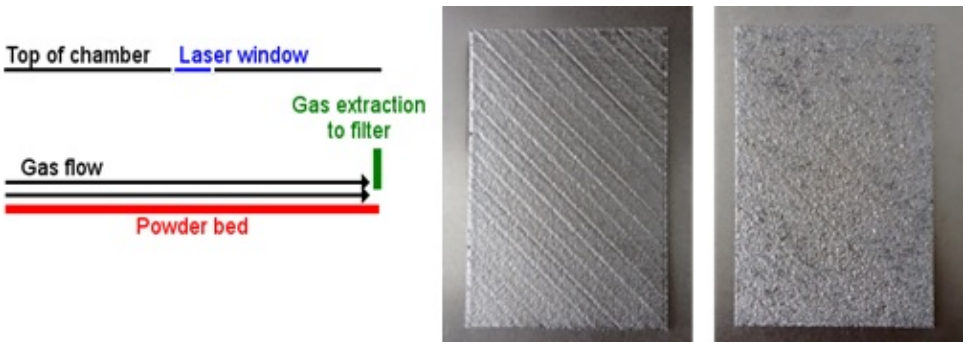

Figure 3 - (a) Schematic showing the gas flow across the powder bed; (b) comparison of surface roughness of parts printed with optimized flow (left) and bad flow (right) conditions

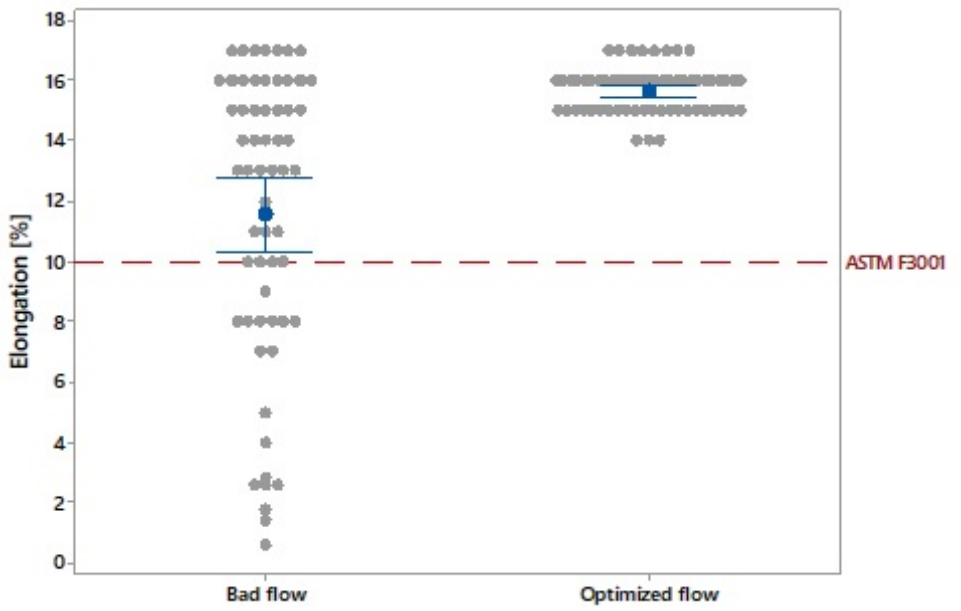

Figure 4-Comparison of elongation properties obtained by tensile testing of samples printed with bad flow and optimized flow

The graph clearly indicates that the samples printed under a bad flow condition show a large spread in the ductility and lower values than the samples printed in an optimized flow condition. The bad values are again attributed to spatters and its effect on the formation of the non-fusion defects. The recent works from Bisht et al. [13] and Coeck et al. [14] report findings using in-situ monitoring of melt pool using DMP monitoring, which proofs that bad flow conditions across the powder bed lead to the formation of spatter induced non-fusion pores and thus having a significant impact on the final mechanical properties.

Homogeneity across build plate

For serial manufacturing or manufacturing of large parts, it is important that the quality is repeatable across the whole platform. This can be achieved by having a robust optical train and a homogeneous gas flow across the build area. With a defined process protocol, the DMP ProX® 320 system can be maintained robust and in turn produce a repeatable and fine print quality. A test was designed in order to evaluate the robustness of the print quality across the build platform. A representative 3DXpert™ build platform which contained the parts used for testing are shown in Figure 5

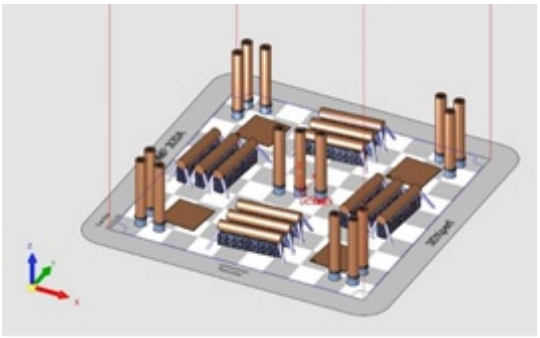

Figure 5-Representive build lay-out as seen in 3Dxpert™

Density

Density is the primary property to give the first indication about the quality of the printed parts. It can be evaluated using Archimedes' principle and metallography pixel count method. In this study, only Archimedes' method was used for which a theoretical density of 4.43 g/cm^3 was taken. Standard 10x10x10 mm^3 size density cubes were printed across the build plate at different locations using different layer thicknesses - LT 30, LT 60 and LT 90 with standard LaserForm parameters and optimized flow settings. The obtained results are shown in Figure 6. The positions - 1, 3, 7 and 9 correspond to Rear Left, Rear Right, Front Left and Front Right across the build platform. The results clearly indicate that the density of the printed parts stays stable across the build platform at around 99.3 %. The variance is well within the 95% CI and further this asserts the homogeneity of the printing quality across the build platform. The results indicate that HIP might not be necessary and the as-printed samples could already exhibit the desirable density properties. It should be taken in to account that the Archimedes' method of testing is not accurate and thus 100 % density cannot be measured for any part.

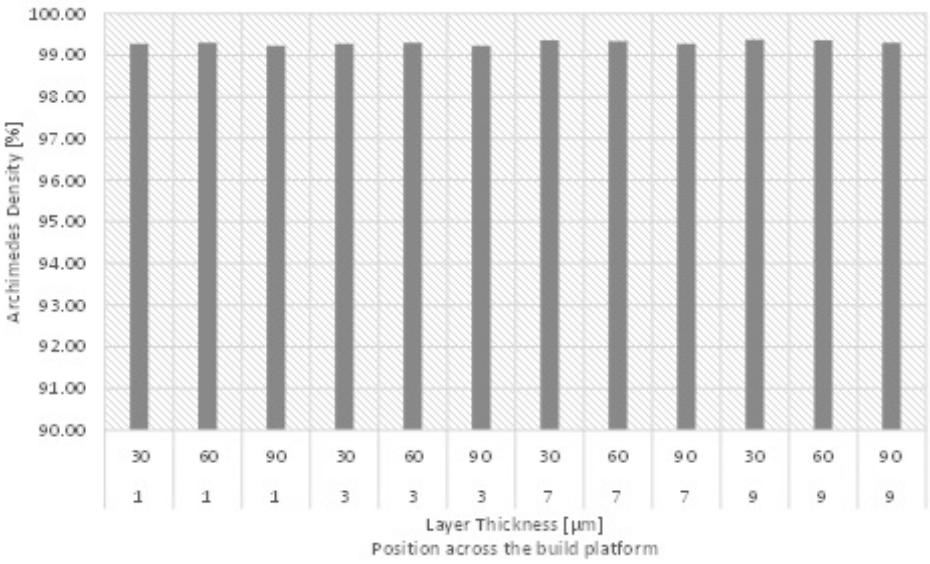

Figure 6-Archemedes density of cubes printed using LT 30, 60 and 90 µm at 4 different locations

The good part density, low oxygen content and fine-tuned microstructure lead to a good combination of strength and ductility, which will be discussed in the next section. Thus, thorough machine and process optimization, the print homogeneity across the build platform and minimal print-to-print variations are achieved.

Mechanical properties

Tensile tests

The most important parameter to evaluate the homogeneity across the build platform is the mechanical properties. In Figure 7, the yield strength, ultimate tensile strength and elongation values of LT 30, 60 and 90 samples (stress relieved and machined) averaged across all the 9 different positions are plotted in comparison with the ASTM F3001 standards. The results give a clear indication that the obtained properties are well above the required standards. Figure 8 shows the difference in elongation obtained at different positions across the build plate for different layer thicknesses. In general, the elongation values are very stable across the build platform irrespective of the used layer thickness. LT 90 properties show slightly a higher spread compared to LT 60 and LT 30 but on the upper side and so is not a negative observation. In general, the good strength-ductility combination can be attributed to the fine-tuned process parameters and machine architecture that helped to achieve defect minimal parts as well as the good choice of stress relieve heat treatment. Rapid solidification of the L-PBF process

features a very fine microstructure in the as-printed Ti-6Al-4V. The tailored SR heat treatment relieves residual stresses and decomposes the brittle acicular martensitic phase into a fine α+β Widmanstätten microstructure. This produces an excellent combination of strength-ducility. A detailed article on this study is still under preparation.

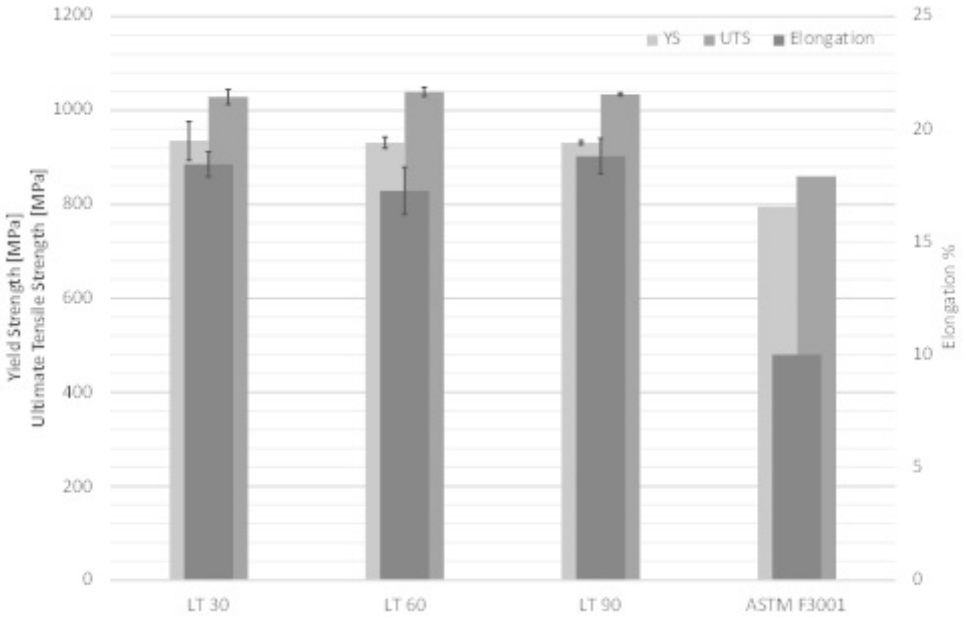

Figure 7-Comparison of mechanical properties with ASTM F3001 standards

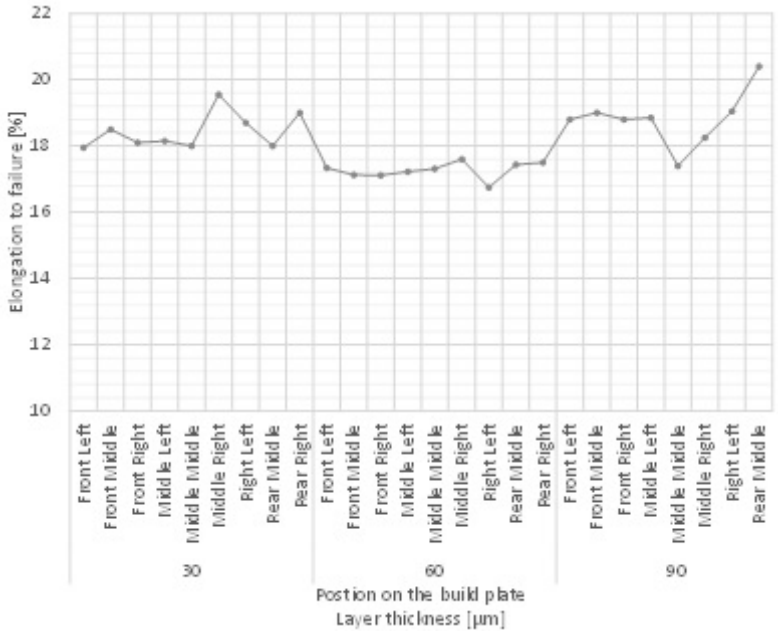

Figure 8-Comparison of elongation properties between 30, 60 and 90 µm LT samples printed at different build positions

Fatigue tests

Fatigue is another important property relevant for several structural applications and highly sensitive for small defects. AM, in general has been seen sceptic for manufacturing parts for fatigue critical applications. This is mainly attributed to the process induced defects that can be caused by several factors which were briefly discussed in previous sections. In this study, we have established that such process induced defects can be avoided almost completely and obtain a homogeneous and repeatable print quality without necessity for HIP. Alongside these defects, there are other factors that contribute to the fatigue properties – microstructure and surface roughness. Microstructure is defined by the type of phases being present in the material. In the as-printed condition, Ti-6Al-4V has alpha' – brittle martensitic microstructure. After the SR treatment, a fine α+β Widmanstätten microstructure is formed which is highly beneficial for the fatigue properties. Therefore the combination of robust, repeatable part quality and tailored heat treatment provide good fatigue properties. Cutolo et al [3] reports this finding and even concludes that the SR treatment helps in achieving a better fatigue properties than HIP. The other important parameter for fatigue properties is surface roughness. Surface roughness plays a major role in the time needed for the crack to initiate. Therefore, to obtain best fatigue

properties, the samples/parts need to post machined to surface roughness values below 0.5 Ra [um]. Fatigue tests were performed on machined samples according to ASTM E466 specifications and tested in a tension-tension mode (R=0.1). The results can be seen in Figure 9. It could be noticed from the graph that the fatigue limit is at around 657 MPa ($5x10^{-6}$ cycles). This results is very much comparable or even better than cast Ti-6Al-4V results reported in Li et al. [2] and one of the best that could be seen from literature for L-PBF processed Ti-6Al-4V [2,3].

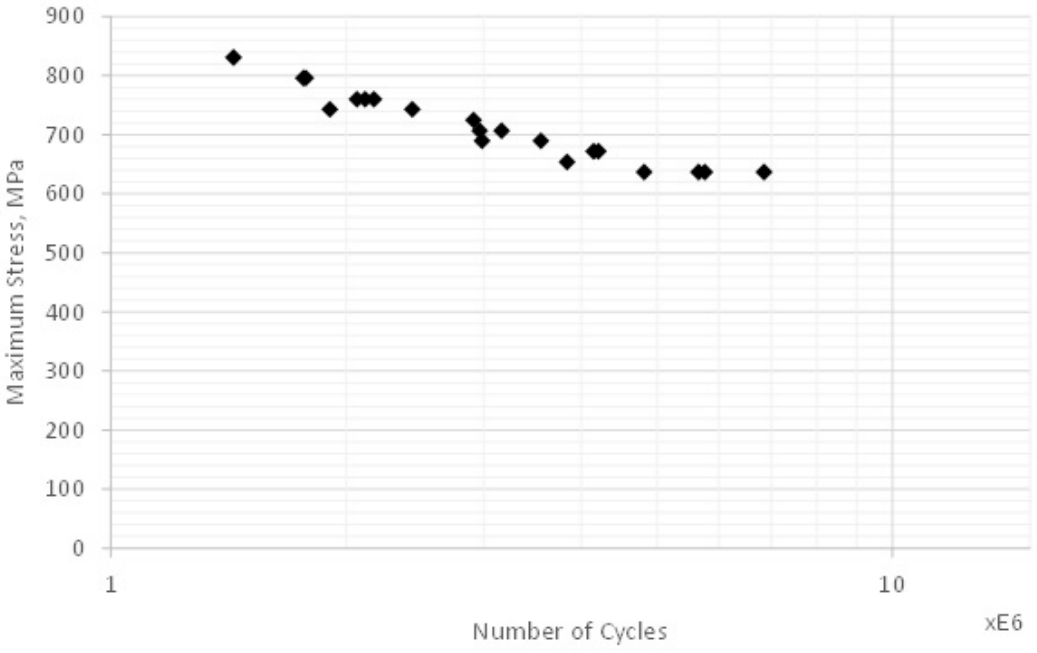

Figure 9-SN curve of LaserForm® Ti Gr23 tested in tension-tension (R=0.1)

Conclusions

A critical assessment on the homogeneity of mechanical properties and build quality of LaserForm™ Ti Gr23 across build plate was performed on a DMP ProX 320 machine. The excellent atmospheric control using robust machine architecture, optimized gas flow, fine-tuned process parameters and choice of a tailored heat treatment make it possible to obtain reliable and repeatable print-to-print quality with very good strength-ductility combination and excellent fatigue properties without the use of HIP.

References

[1] T. DebRoy, H.L. Wei, J.S. Zuback, T. Mukherjee, J.W. Elmer, J.O. Milewski, A.M. Beese, A. Wilson-Heid, A. De, W. Zhang, Additive manufacturing of metallic components – Process, structure and properties, Prog. Mater. Sci. 92 (2018) 112–224.

[2] P. Li, D.H. Warner, A. Fatemi, N. Phan, Critical assessment of the fatigue performance of additively manufactured Ti – 6Al – 4V and perspective for future research, 85 (2016) 130–143.

[3] A. Cutolo, C. Elangeswaran, C. De Formanoir, G.K. Muralidharan, B. Van Hooreweder, Effect of Heat Treatments on Fatigue Properties of Ti – 6Al – 4V and 316L Produced by Laser Powder Bed Fusion in As-Built Surface Condition, (n.d.) 395–405.

[4] M. Yan, W. Xu, M.S. Dargusch, H.P. Tang, M. Brandt, M. Qian, Review of effect of oxygen on room temperature ductility of titanium and titanium alloys, Powder Metall. 57 (2014) 251–257.

[5] J.M. Oh, B.G. Lee, S.W. Cho, S.W. Lee, G.S. Choi, J.W. Lim, Oxygen effects on the mechanical properties and lattice strain of Ti and Ti-6Al-4V, Met. Mater. Int. 17 (2011) 733–736.

[6] R. Li, J. Liu, Y. Shi, L. Wang, W. Jiang, Balling behavior of stainless steel and nickel powder during selective laser melting process, Int. J. Adv. Manuf. Technol. 59 (2012) 1025–1035.

[7] H. Nakamura, Y. Kawahito, K. Nishimoto, S. Katayama, Elucidation of melt flows and spatter formation mechanisms during high power laser welding of pure titanium, J. Laser Appl. 27 (2015) 032012.

[8] I. Yadroitsev, P. Krakhmalev, I. Yadroitsava, S. Johansson, I. Smurov, Energy input effect on morphology and microstructure of selective laser melting single track from metallic powder, J. Mater. Process. Technol. 213 (2013) 606–613.

[9] M.J. Matthews, G. Guss, S.A. Khairallah, A.M. Rubenchik, P.J. Depond, W.E. King, Denudation of metal powder layers in laser powder-bed fusion processes, in: Addit. Manuf. Handb. Prod. Dev. Def. Ind., 2017.

[10] S. Li, G. Chen, S. Katayama, Y. Zhang, Relationship between spatter formation and dynamic molten pool during high-power deep-penetration laser welding, Appl. Surf. Sci. 303 (2014) 481–488.

[11] S. Ly, A.M. Rubenchik, S.A. Khairallah, G. Guss, M.J. Matthews, Metal vapor micro-jet controls material redistribution in laser powder bed fusion additive manufacturing, Sci. Rep. 7 (2017) 1–12.

[12] V. Gunenthiram, P. Peyre, M. Schneider, M. Dal, F. Coste, I. Koutiri, R. Fabbro, Experimental analysis of spatter generation and melt-pool behavior during the powder bed laser beam melting process, J. Mater. Process. Technol. 251 (2018) 376–386.

[13] M. Bisht, N. Ray, F. Verbist, S. Coeck, Correlation of selective laser melting-melt pool events with the tensile properties of Ti-6Al-4V ELI processed by laser powder bed fusion, Addit. Manuf. (2018).

[14] S. Coeck, M. Bisht, J. Plas, F. Verbist, Prediction of lack of fusion porosity in selective laser melting based on melt pool monitoring data, Addit. Manuf. (2019).